NUKLEONIKA 2002;47(4):155–162

ORIGINAL PAPER

Influence of powerful pulses of hydrogen plasma upon materials in PF-1000 device

**Valery N. Pimenov,
Vladimir A. Gribkov,
Alexander V. Dubrovsky,
Franco Mezzetti,
Marek Scholz,
Yulo E. Ugaste,
Elena V. Dyomina,
Lev I. Ivanov,
Sergey A. Maslyaev,
Ryszard Miklaszewski,
Michal Borowiecki,
Paola De Chiara,
Linda Pizzo,
Adam Szydlowski,
Igor V. Volobuev**

Abstract The results of experimental investigations of powerful hydrogen plasma jets and fast ion beams interaction with various materials (austenitic chromium-manganese steels, pure vanadium, tungsten, graphite, copper, and their alloys: Cu-4 mass% Ni and Cu-10 mass% Ga) are presented. The materials were placed on the discharge axis of the PF-1000 device and irradiated with fluxes of fast ions (of energy in the range from tens keV up to several MeV) and with plasma streams (of power flux density q~(10^8–10^9) W/cm^2). It was found that the fast ions and plasma streams caused different damages to the aforementioned materials. A diverse character of the damages to the individual investigated material was revealed. Some peculiarities of the process as well as the correlation between the surface density of the "macroscopic" structural defects (blisters and craters) and the fluence of the fast ions implanted in the specimen are discussed.

Key words dense plasma focus • ion beam • irradiation • plasma jet • surface damage • test specimen

V. N. Pimenov✉, E.V. Dyomina, L. I. Ivanov,
S. A. Maslyaev
A. A. Baikov Institute of Metallurgy and Material Science,
Russian Academy of Sciences,
49 Leninsky Pr., 117334 Moscow, Russia,
Tel.: 7 095/ 135 9604, Fax: 7 095/ 135 8680,
e-mail: pimenov@ultra.imet.ac.ru

V. A. Gribkov, M. Scholz, R. Miklaszewski, M. Borowiecki
Institute of Plasma Physics and Laser Microfusion,
23 Hery Str. 00-908 Warsaw, Poland

A. V. Dubrovsky, I. V. Volobuev
P. N. Lebedev Physical Institute,
Russian Academy of Sciences,
53 Leninsky Pr., 117924 Moscow, Russia

F. Mezzetti, P. De Chiara, L. Pizzo
University of Ferrara, INFM,
12 Via Paradiso, I-44100 Ferrara, Italy

Y. E. Ugaste
Pedagogical University of Tallinn,
25 Narva Road, 10120 Tallinn, Estonia

A. Szydlowski
The Andrzej Soltan Institute for Nuclear Studies,
05-400 Otwock-Swierk, Poland

Received: 22 May 2001, Accepted: 28 June 2002

Introduction

This paper presents studies on the influence of powerful plasma streams upon various materials and is a continuation of our previous work performed with the Plasma-Focus device. Methodological aspects of the experiments with the PF-1000 device were described in [2, 16]. In this paper presented are some results of the study on combined influence of X-ray radiation, high-energy hydrogen ions, high-temperature dense plasma streams, and a shock wave on the materials irradiated within the PF-1000 installation. The basic scientific results obtained from the irradiated specimens will be discussed in this paper.

It has been shown, in our previous papers [5, 6, 13] that a complex interaction of nano- and microsecond fast ion beams, X-ray radiation, and deuterium plasma jets (in a wide range of power flux density; q=(10^7–10^{12}) W/cm^2 upon the materials in question results in significant damages also to surface modification of the irradiated material specimens. It was found that characteristic features of the specimen surface interaction with the radiation emitted from PF-discharges strongly depend on the irradiation regime i.e. on power flux density q, pulse duration τ, the delay between the fast ions and plasma jet intensity peaks Δt, the distance between the anode face and the specimen h etc. In particular, so-called "detachment" effect (formation of a cold plasma cloud nearby the surface of the irradiated sample) readily occurs at q=(10^8–10^9) W/cm^2, and a "broken" implantation regime appears to a the role under a high power density q=(10^9–10^{11}) W/cm^2. The implantation of high energy ions (E_i≈100 keV) was observed at the relatively low power density q=(10^7–10^8) W/cm^2. In those experiments (with q relatively low), the distance h was chosen to be small, so that all the above mentioned types of hard radiation interacted almost simultaneously (Δt=0).

Table 1. Specimens tested in the PF-1000 experiment.

Material	Chemical contents of test material (mass%)	Specimen form	Specimen dimensions (mm)	Specimen manufacturing method
Steel 25Cr12Mn20W	0.25-C, 12-Cr, 20-Mn, 1-W	Plate	15×15	Fusion, rolling
Steel 10Cr12Mn20W	0.1-C, 12-Cr, 20-Mn, 1-W	Plate	15×15	Fusion, rolling
Technical copper	99.5%Cu	Tablet	⌀12	Fusion, rolling, cutting, grinding
Alloy copper + nickel	Cu + 4%Ni	Tablet	⌀10	Fusion, cutting, grinding
Alloy copper + gallium	Cu + 10%Ga	Tablet	⌀10	Fusion, cutting, grinding
Vanadium alumo-thermal	99.4%V	Tablet	⌀12	Fusion, rolling, grinding
Tungsten single crystal		Tablet	⌀15	Guiding crystallization, el.-erosive cutting, grinding
Carbon high-purity		Tablet	⌀12.5	Cutting, grinding

The aim of this work was to investigate the characteristic features of the material damages caused by pulsed fluxes of fast hydrogen ions and plasma streams at two special irradiation conditions:

- with a significant delay Δt (approximately a few microseconds) between the high energy hydrogen ion fluxes and the plasma jets,
- when the main part of the incident energy is delivered to the specimens by the plasma jets.

These two regimes made it possible to separate the contribution of two effects to the damages of the irradiated specimen; the effect caused by radiation and the one caused by heat impact. This separation was possible both in time and in the energy content. It facilitated the interpretation of the results of the integral action of both the factors.

Materials

The investigated, shape and sizes of the specimens as well as their preparation techniques are presented in Table 1. The investigated materials were selected taking into consideration that austenitic chromium-manganese steels, pure vanadium, tungsten, graphite, copper, and their alloys are of significant resistance and stability when undergone high thermal and radiation loading [1, 8, 14]. Besides, these materials are rigid against corrosion and exhibit good mechanical properties [4, 11, 12, 19]. All the above mentioned properties make them the most suitable and perspective for structural and functional materials undergoing high-power pulsed radiation in energy loaded components of modern high-temperature plasma and other related facilities. Previously considered "candidate" – materials were tested in the experiments performed with a DPF device which was equipped with a flat anode and was operated with deuterium gas [5, 6, 13].

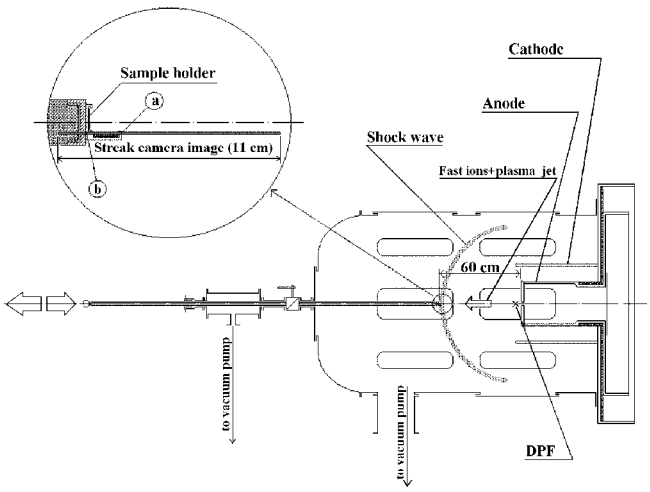

Fig. 1. A scheme of the PF-1000 experiment.

Steels under investigation were melted, rolled up to 0.1 cm thickness and prepared as plates for the experiments performed with the PF-1000 device (see their dimensions in Table 1). Specimens of pure vanadium, tungsten, graphite, and copper-based alloys were prepared as disks of 1.5–2 cm in diameter (see Table 1).

Experimental methods and analysis

Experiments with the PF-1000 device

A scheme of the experiment is presented in Fig. 1. The electrical energy stored in the capacitor bank of the PF-1000 device amounted to 580 kJ. The discharge chamber was filled with pure hydrogen under an initial pressure of 200 Pa. The sample holder was fixed on the tip of a long metallic arm. A final fragment of the arm, 10 cm long, has been made of plastic insulator. A distance from the plasma focus (the source of radiation) to the specimen was 60 cm. Discharge current was measured with a Rogowski coil and attained 1.5 MA. A Roentgen-Gamma dosimeter of the 27040 type (ionization chamber with a spectral range of 8 keV – 3 MeV) was used to measure an X-ray radiation dose in every DPF discharge. Fast ion fluxes intercepted by the test specimen were determined using a solid state nuclear track detector of the CR-39 type. The detector sample were located close to the test specimen on the same sample holder. A fast streak camera was used to record the hot plasma jet interaction with the specimen. More detail description of the PF-1000 facility and the diagnostic tools one can find in [2, 16]. The specimens were placed on the holder in this way that they were irradiated at normal incidence of the radiation to the sample surface. All the specimens, excluding the 10Cr12Mn20W steel, were irradiated with three pulses in series. The specimens of 10Cr12Mn20W steel were irradiated with 3, 6, and 10 pulses in series. Power flux density of the plasma jets ranged from 10^8 to 10^9 W/cm^2 and the pulse duration τ was about 10^{-6} s.

Methods of analytical investigation of the specimens

After irradiation, the specimens were investigated under an optical and scanning electron microscope. Besides of this, an X-ray diffraction analysis (at Ferrara University), an X-ray

spectral analysis, and an X-ray diffraction analysis with an optical microscopy (the A. A. Baikov Institute in Moscow, Russia in cooperation with the Pedagogical University in Tallinn, Estonia) were used to study the surfaces of both irradiated and non-irradiated specimens.

The comparative qualitative analysis of the carbon and oxygen contents in the primary (non-irradiated) and irradiated specimens of austenitic chrome-manganese steels has been carried out by means of the method of local X-ray spectral analysis of light elements [10]. The diamond and silicon dioxide (SiO_2) were used as standards for carbon and oxygen analysis, respectively. The content of the studied element was evaluated on the basis of the signal amplitude from an X-ray detector (proportional counter) with respect to the signal from the standard. The counting time was equal to 10 s for each studied point on the specimen surface. The depth of the analyzed layer was about 1 μm. The thickness of the layer, which was evaporated during the irradiation of the specimen with high energy ions and plasma jets was determined by the method of precise weighing of the test sample before and after its exposure.

Results and discussion

Evaporation of the surface layers

The weighing of the primary and irradiated samples has revealed that the irradiation of the specimen led to intensive evaporation of its external layer. The thickness of the layer that evaporated after a single DPF shot d appeared to be less than the mean free path of the fast ions in the tested materials R (if e.g. E_i=100 keV, then $R \leq 1$ μm [14]). Precisely speaking, it was found that the relation between the parameters d and R varied in the range $0.2\,R \leq d \leq R$. In particular, the layer removed was almost equal to the mean free path of the ions in the samples in the case of pure vanadium as well as Cu-4 mass% Ni and Cu-10% Ga alloys. In these circumstances, the implanted ions were extracted from the material practically completely, together with the evaporated layer ("broken implantation" regime [5]). In that case deeper layers were subjected only to thermal influence. On the contrary, if $d<R$, the implantation of fast ions of energy 70 keV $\leq E_i \leq$ 130 keV was found to occur at the depth $\sim(R-d)$.

The relationship between the values of d and R for austenitic chrome-manganese steels was $d \cong 0.37\,R$.

Under the described experimental conditions the effect of cumulative plasma jet upon the sample surface was delayed in relation to the impact of fast ions by about $\Delta t \sim (6–8)$ μs. In these experiments the power flux density of fast ions was evaluated to be only $q \sim 10^{-2}$ W/cm^2, whereas the plasma jet power was $\sim 10^8$ W/cm^2 [2]. In other words, the bulk energy of the interaction was transported to the sample by the cumulative plasma jet, which produced a strong thermal impact upon the surface even though its penetration depth was low ($R<10$ nm) [14]. Thus, this jet let to the surface evaporation and to the surface burn-off processes. Moreover, a shock wave running through the material volume was induced. On the contrary to that, the plasma jet did, the fast hydrogen ions produced cascades of atomic collisions inside the material volume [17].

The surface damage

The test samples, which were analyzed before and after the pulsed energy interaction have revealed that the implantation of high-energy hydrogen ions to the sample material took place. The strongly displayed phenomena of melting, evaporation, and sputtering of the surface layer have been registered. The flowing surface of the irradiated materials had often a wavy nature and included craters, blisters, and micro-cracks. Nevertheless, some irradiated samples retained the surface plane enough. On the whole, the damage character as well as the type of modification of topographic surface structure of the tested materials have some distinctive properties, which we shall discuss below.

The photos taken with an electron beam scanning of the primary and irradiated surfaces of the 25CrMn20W steel specimens are presented in Fig. 2. It is seen on these photos that the surface irradiated with 3 pulses contains an ample quantity of relatively deep craters of diameter f up to 10 μm, small blisters ($f \leq 1$ μm), and also micro-craters. It should be emphasized that the majority of the craters is situated on the convex part (crests) of the surface. One should notice that the 10Cr12Mn20W steel surface has different damage character than the other specimens. It shows a substantial number of

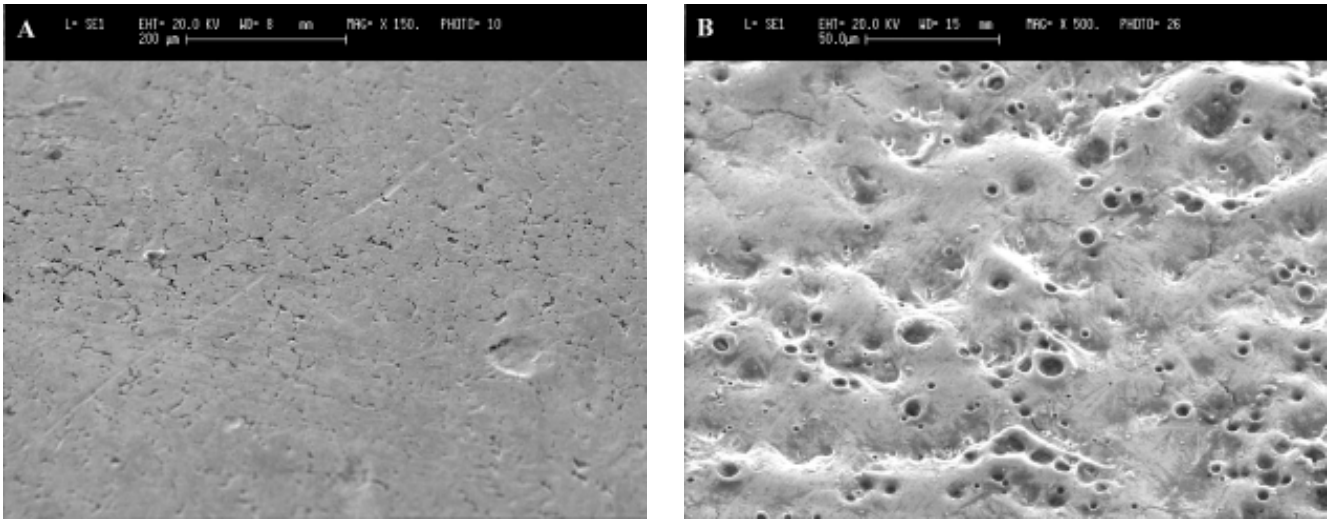

Fig. 2. The electron scanning of the part of 25Cr12Mn20W steel sample surface. A – initial state; B – after 3 pulses of the hydrogen plasma actions. Wavy nature of the surface containing craters, small blisters, and micro-cracks is visible.

Table 2. Density of the structural defects on the irradiated material surface after experiment in the PF-1000 device.

No.	Material pulses	Basic defect type ρ, 10^5 cm^{-2}	Number of radiation	Surface density of defects
1	25Cr12Mn20W	Craters	3	2.0
2	25Cr12Mn20W	Craters	3	3.0
3	10Cr12Mn20W	Blisters	6	5.3
4	10Cr12Mn20W	Blisters, craters	8	6.2
5	Technical Cu	Craters	3	5.5
6	W	Craters, micro-cracks	3 0.9	12.0

Table 3. Carbon and oxygen content in 10Cr12Mn20W steel samples (qualitative analysis).

No.	Material	Test sample	X-ray pulses meter-reading for 10 s	
			Carbon	Oxygen
1	Diamond	Standard	26,010; 25,970; 26,100; 25,890; 26,050	–
2	SiO_2	Standard	–	16,360; 16,800; 16,640; 14,550; 14,230
3	10Cr12Mn20W	Initial sample (light-colored field)	75; 76; 58; 64; 73	78; 76; 75; 80; 83
		Irradiated sample (8 act.) (light-colored field)	29; 32; 36; 44; 43 50; 52; 52; 53; 49	40; 42; 47; 41; 45; 40;
4	10Cr12Mn20W	Irradiated sample (8 act.) (bubbles)	1) 204; 194; 190; 196; 198 2) 116; 120; 135; 129; 137 3) 268; 257; 256; 276; 277 4) 173; 186; 194; 201; 210 5) 319; 301; 312; 322; 300 6) 242; 253; 245; 271; 281	1) 369; 382; 390; 393; 359 2) 252; 393; 409; 428; 412 3) 197; 213; 342; 234; 243

relatively large blisters ($f \leq 10$ mm) and a small number of craters.

The average surface density ρ of structure defects (the number of defects per unit area) has been determined for the austenitic steels (under investigation) as well as for copper and tungsten. The results are present in Table 2. The determined density values (Table 2) are in good correlation with the fast (70 keV $\leq E_i \leq 130$ keV) hydrogen ion fluence, which has been implanted into the irradiated specimen, and which has been measured by track detectors [15]:

$$\rho \cong (0.6\text{–}2.0) \times 10^5 \text{ defects/cm}^2$$

This means that the macroscopic surface density of the defects is in good correlation with the density of the microparticles, i.e. hydrogen ions hitting the specimen.

It is reasonable to assume that the high energy hydrogen ions, which were implanted to the depth $R = 0.5$ μm, influenced the formation of the obtained surface structural defects i.e. craters and blisters. The results of the analyses of the carbon and oxygen contents within thin surface layers (up to ~1 μm) confirm this assumption (Tables 3 and 4). It is seen (Table 3) that the redistribution of both the gas components takes place in the surface layer of the 10Cr12Mn20W steel specimen already after the irradiation. Some decrease of the carbon as well as oxygen contents is observed in the bulk volume of the alloy, while the generated blisters revealed an evident increase of these components. It is justified to suppose that the blisters are filled with carbon- or/and oxygen-containing gases (i.e. CO, CO_2, O_2) or possibly with more complicated gas compounds. According to the data obtained (Table 4) the irradiation caused a noticeable increase of the carbon and oxygen contents in the surface layer of the 25Cr12Mn20W steel specimens. In addition, the most remarkable growth of the concentration of both the components usually was obtained in the relief surface parts located close to the craters (on the "crests" of the wavy surface). Note that the majority of the craters are also located on the relief part of the specimen.

Table 4. Carbon and oxygen content in 25Cr12Mn20W steel samples (qualitative analysis).

No.	Material	Test sample	X-ray pulses meter-reading for 10 s	
			Carbon	Oxygen
1	Diamond	Standard	26,080; 26,020; 26,100; 25,990; 26,030	–
2	SiO_2	Standard	–	16,340; 16,090; 16,050; 15,920
3	25Cr12Mn20W	Initial sample (light-colored field)	310; 555; 403; 361; 428; 456	378; 488; 527; 501; 518
4	25Cr12Mn20W	Irradiated sample (3 act.)		
		(light-colored field)	536; 639; 640; 730	476; 514; 500; 495
		(drop)	2700; 2580; 2540; 2520; 2626	1597; 1480; 1506; 1350
		(dark spot no. 1)	790; 798; 768; 833; 894	744; 843; 788; 767; 776
		(dark spot no. 2)	7768; 7934; 7807; 7952; 7827	–

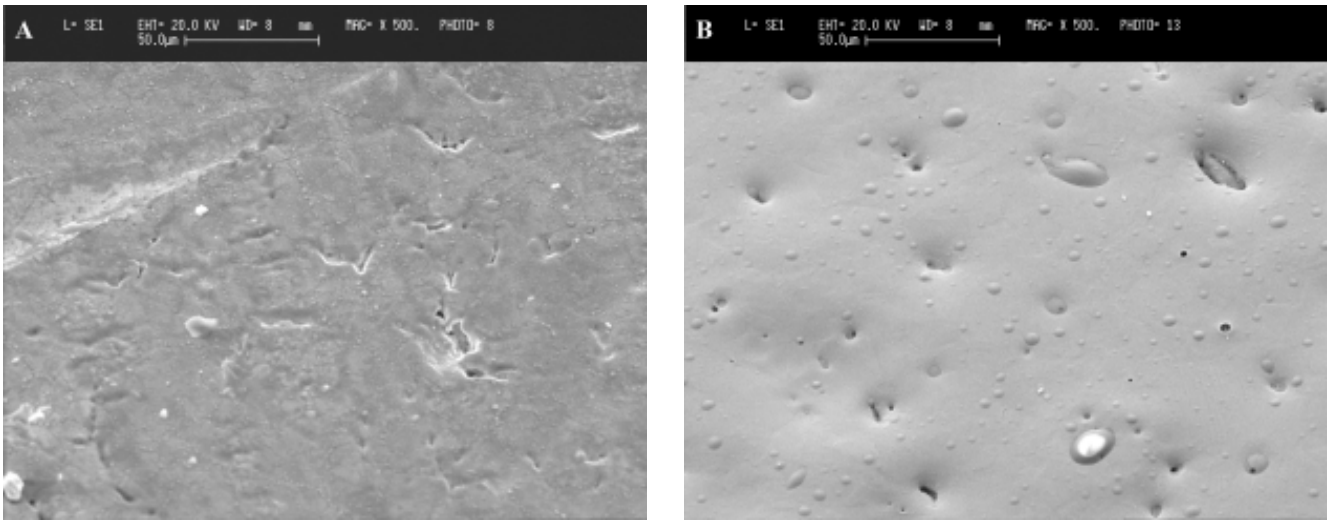

Fig. 3. The electron scanning of the part of 10Cr12Mn20W steel sample surface. A – initial state; B – after 8 pulses of the hydrogen plasma actions. Wavy nature of the surface containing multitude blisters and some craters is visible.

Moreover, an increase of the carbon content above the normal level is usually observed in some surface fragments looking like dark spots. Apparently, the fragments represent carbides of the elements (which constitute parts of the steel) or more complicated compounds containing carbon. Basing on the results obtained for the austenitic steel, one can suggest that the radiation defects (the cascades of atomic collisions produced by the implantation of hydrogen ions into the test samples) represent a vacancy cloud – "vacancy clusters" – of the characteristic linear dimension $L \cong 1$ μm [20, 21]. The clusters (microvoids) constitute stable embryos of the gas phase, which is created subsequently inside the near-surface zone of the solid material. Indeed, later on (by a few micro-seconds), during the process of powerful thermal influence of the cumulative plasma jet, the mater surrounding the considered embryos is transformed into the liquid phase. Working as effective drains for carbon and oxygen atoms, they grow fast enough to produce bubbles – due to transformation of the above mentioned atoms from the liquid to gaseous phase. The intensive mass transfer of the components by the thermal capillary (cellular) convection, developing in the field of temperature gradient on the interface of the solid and liquid phase, i.e. on the bubble shell, promotes this process [13]. The melt content, as well as the specific temperature and time dependent conditions, determine gas content of the gaseous phase. This gas quickly migrates towards the heated surface of the specimen. Comparing the 25Cr12Mn20W and 10Cr12Mn20W types of steel one can conclude that the last one, having less initial C and O contents (Tables 3 and 4) reveals more shaped blisters in the surface layer (Figs. 3 and 4). With regard to the 25Cr12Mn20W steel, which includes more initial C and O contents, the gas bubbles are formed within the liquid phase evidently under a higher pressure, which destroys the bubble shells and produces defects of the crater type. In both cases the process of bubble formation in the surface layer promotes the constitution of the wavy nature of the irradiated sample surface.

The specimens of pure vanadium showed a quite different nature of the surface damages. The irradiated surface did not demonstrate the characteristic wave shape and after 3 irradiating pulses it looked fairly smooth. The surface practically had neither craters nor blisters, although it had many extensive micro-cracks. As it was mentioned above, the thickness of the vanadium layer that was evaporated by a single pulse of plasma is $d \approx R$ (R – range of hydrogen ions of energy $E \approx 100$ keV). One can conclude that in this case initially implanted ions as well as the defects induced by these ions were practically removed from the material as a result of evaporation of the surface layer by the subsequent plasma jet. Thus, the so called "radiation factor", which is connected with the generation of atomic collision cascades and which results in the gas phase formation and crater and blister creation (in the case of steel material), was not observed in this case. Due to the same reason the wavy profile of the surface did not appear. It may be thought that the micro-cracks originate as a result of a tension induced by high temperatures. This tension affects the material especially during its fast solidification stage (with a freezing rate of ~(10^8~10^9) degree/s) under the condition of a high temperature gradient (~10^7 degree/cm).

The tungsten (W) specimen demonstrated some specific character of the surface damages after irradiation with 3 pulses. Initially the W specimen held deep traces of electro-erosion

Fig. 4. The electron scanning of the part of 10Cr12Mn20W steel sample surface after 6 pulses of the hydrogen plasma actions. The blisters are visible on the wave like irradiated surface.

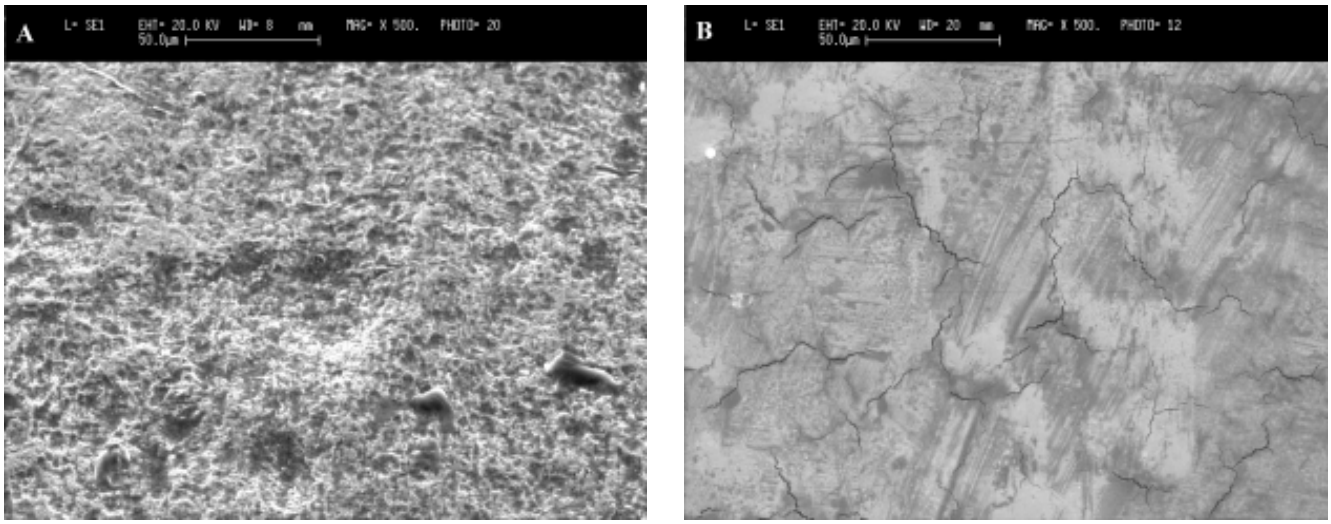

Fig. 5. The electron scanning of the part of the vanadium sample surface. A – initial state; B – after 3 pulses of the hydrogen plasma actions. The irradiated surface is flat enough. It does not contain any wavy zones, craters or blisters. The micro-cracks as well as the islets of deposited copper (as gray degraded spots) are visible.

cutting and grinding. It was notably rough and held micro--cracks and a few craters (Fig. 6). As a result of these procedures of the material processing, carbon and nitrogen were also present in the tungsten specimen [9]. After the irradiation within the PF-1000 device numerous surface imperfections appeared to be more smooth. Besides, a great number of craters and extensive micro-cracks have been formed. A probable reason of crater formation was carbon and nitrogen regress from the material, which was stimulated by the radiation impact of the implanted hydrogen ions and thermal effect of plasma (just as it probably took place in the austenitic steel specimens). The specific topology modification of the post-irradiated tungsten specimen surface resulted from the fact that the depth of its preliminary electro-erosion processing h_0 is greater than the depth of the typical for the PF-1000 experiment ion-plasma impact h_p. Nevertheless, a certain periodicity of the extensive micro-cracks disposition, a specific rolling grade of the surface topology, as well as a large number of rather deep craters (Fig. 6) are of great interest for further investigations.

A proper attention must be paid to the experimental results of the irradiation of the specimens made of "different" copper ("technical" copper, Cu-4 mass% Ni, Cu-10 mass% Ga) (Figs. 7 and 8). The surface of the copper specimen irradiated with 3-pulses contained a large number of craters ($\varnothing \leq 10$ μm) and small blisters ($\varnothing < 1$ μm). On the contrary, the surface of the copper alloy specimens had no craters at all. A few small blisters have been yet observed on their surface. However, it is known that the technical copper contains oxygen as an impurity. The craters on the irradiated surface point out to the process of gas-bubble formation. This process results from the soluble oxygen and extraction of the bubbles through the surface when it is strongly exposed to the heat. The radiation defects produced by the implanted hydrogen ions had stimulated the bubble formation process. In the case of Cu-Ni and Cu-Ga alloys, under the conditions $d \cong R$ ("broken implantation" regime) the so called radiation component of the energy effect turned out to be of less importance for the specimen damage. However, a strong influence of the thermal component of the energy effect (plasma jet) could promote the

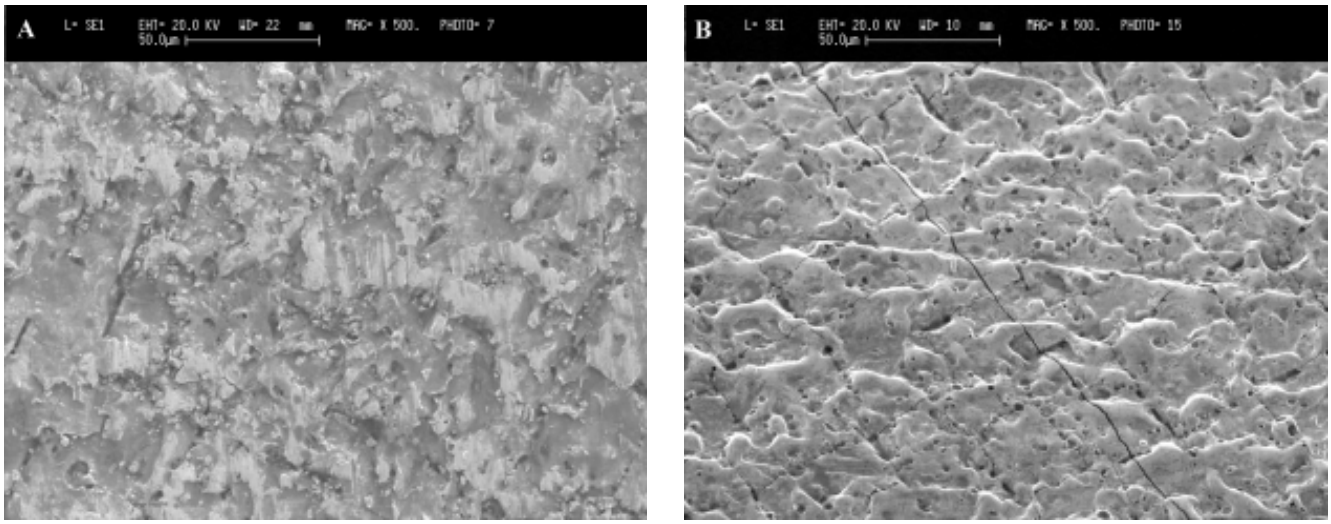

Fig. 6. The electron scanning of the part of the tungsten sample surface. A – initial state (after electro-erosion cutting and grinding; B – after 3 pulses of the hydrogen plasma actions. The traces after cutting – imperfections and micro-cracks are visible. The irradiated surface contains multitude craters and lengthy micro-cracks.

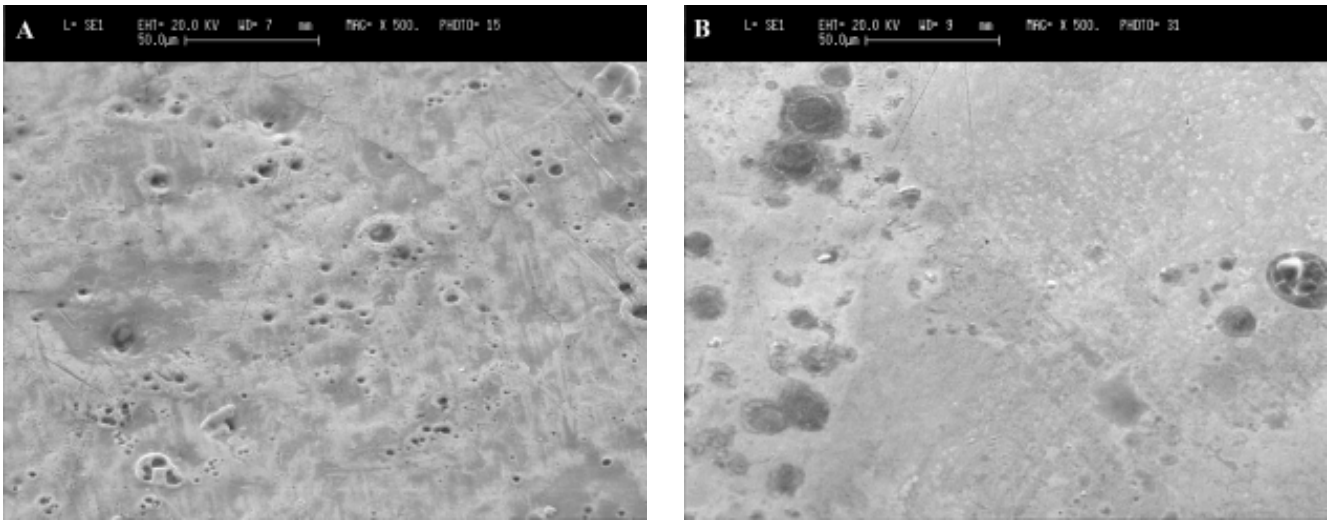

Fig. 7. The electron scanning of the part of the technical copper sample surface – (A) and the Cu-10mass%Ga alloy sample surface – (B) both after 3 pulses of the hydrogen plasma actions. The irradiated surface contains multitude craters and blisters not big in number. One can see the impurities as the dark spots on the surface.

solute gas impurities to diffuse through a free surface of the specimen [7]. Such process usually results in a decrease of the lattice parameter *a* [18]. The values of the parameter *a* were measured by means of the X-ray structural analysis method and are presented in Table 5. According to the data shown in Table 5 the process of gas diffusion caused by the plasma thermal effect is the most remarkable in the case of the Cu-10 mass% Ga alloy.

Contrary to the technical copper specimens, characteristic big formations ($\varnothing \sim 20$–80 mm) are visible as black spots on the surface of the Cu-alloy specimens (Figs. 7 and 8). In order to explain the origin of these spots, a special analysis is needed, which will be carried out later on. It was found in these experiments that the carbon specimens show the highest surface resistance to the action of the pulsed ion beams and plasma jets. Surface character of the carbon specimens practically was not changed by the irradiation (Fig. 9). The more manifested topology of the initial surface structure, developed as a result of dispersion and vaporization processes was the only effect of the irradiation.

The influence of the anode material on the irradiated specimens

Analytical investigations of the specimens have shown that the irradiated surface first of all contains copper. Spatial distribution of the copper along the surface is not homogeneous and an isle structure is observed. In some specimens (e.g. in the V or W ones) the copper is concentrated not throughout the irradiated area, but just in some selected regions. An example of such region is presented on photo in Fig. 5, where the copper formations look like dark blurred spots.

Table 5. The lattice parameter *a* of Cu and based on Cu alloys before and after irradiation of the test samples in PF-1000 device.

Material	The lattice parameter *a* (A)	
	before irradiation	after irradiation
Cu	3.6150	3.6120
Cu-4%Ni	3.6071	3.6054
Cu-10%Ga	3.6405	3.6356

The presence of copper on the irradiated surface is typical for the DPF experiments, since the positive electrode of the device (anode) is manufactured of pure copper. The copper is evaporated from the central part of the anode during every DPF shot and at the final stage of the discharge the copper is deposited on the irradiated specimen surface. Neither physical nor chemical interactions of the deposited copper with the irradiated material were observed, although its adhesion strength is rather high. The deposited film appeared to be resistible enough to the mechanical force which was applied to tear it off from the specimen surface. It was evident that an intensive cleaning of the specimen surface caused by evaporation some of its material, which was performed before the irradiation, led to an increased adhesion strength.

Conclusions

Main types of damages of various materials irradiated under especial exposure conditions (fast hydrogen ions interacted with the specimen a few microseconds earlier than the plasma jet) within the PF-1000 facility were determined.

Fig. 8. The electron scanning of the part of the Cu-4mass%Ni alloy sample surface after 3 pulses of the hydrogen plasma actions. One can see the impurities as the dark spots on the surface.

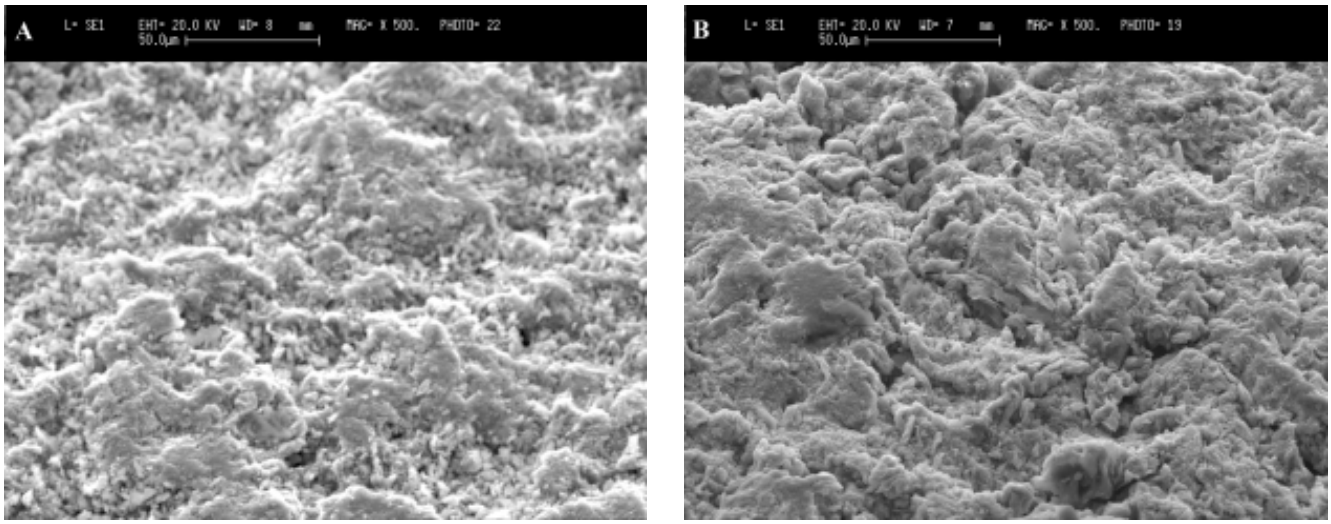

Fig. 9. The electron scanning of the part of the carbon sample surface. A – initial state; B – after 3 pulses of the hydrogen plasma actions. One can see that the surface nature has not been changed as a result of irradiation.

Different character of the surface damages of the investigated materials irradiated under given exposure conditions was revealed.

In some material specimens (austenitic steel, tungsten), a modified layer with a wave surface topology was induced under these exposure conditions. Also new specific effects were observed for the first time.

This phenomenon consists in the fact that the surface density of structure defects (blisters and craters) is related to the fluence of fast (E~100 keV) hydrogen ions implanted into the specimen.

The observed effect points at the non-traditional mechanism of the topology formation: the defect and phase structure of the superficial-surface layer. It is connected with the specific interaction of the radiation and thermal components of the exposure pulse, which influence the material under investigation.

Acknowledgments This work was supported in part by INCO-COPERNICUS (Contract no. ERB IC 15-CT98-0811), the International Atomic Energy Agency (Contracts nos.: 11940/R0, 11941/R0, 11942/R0, 11943/R0, and 12062/R0) and FOP "Integration" (Project no. A-098/2001).

References

1. Abe F, Garner FA, Kayano H (1994) Effect of carbon on irradiation hardening of reduced-activation 10Cr-30Mn austenitic steels. J Nucl Mater 212-215:760–765
2. Borowiecki M, De Chiara P, Dubrovsky AV *et al.* (2001) Experimental study of a powerful energy flow effect on materials in PF-1000 installation. Nukleonika 46;S1:117–122
3. Burtsev VA, Gribkov VA, Filippova TI (1981) High-temperature pinch phenomena. Itogi Nauki i Tekhniki. Fizika Plazmy 2:80–137 (in Russian)
4. Ivanov LI, Maslyaev SA, Pimenov VN (1999) The use of liquid metals in porous materials for diverter applications. J Nucl Mater 271-272:405–409
5. Ivanov LI, Pimenov VN, Dyomina EV *et al.* (2000) Interaction of high temperature deuterium plasma streams with condensed materials in dense plasma focus device. In: 14th Int Conf on Plasma Surface Interactions in Controlled Fusion Devices. Rosenheim, Germany, p 3.51
6. Ivanov LI, Pimenov VN, Maslyaev SA *et al.* (2000) Influence of dense plasma pulses on materials in Plasma Focus device. Nukleonika 45;3:203–207
7. Ivanov LI, Ugaste YE, Pimenov VN *et al.* (2000) Mass transport of hydrogen from iron based alloys to outside environment. Perspektivnye Materialy 2:18–24 (in Russian)
8. Klueh RL, Kenik EA (1994) Thermal stability of manganese-stabilized stainless steels. J Nucl Mater 212-215:437–441
9. Kovalenko VS, Verkhoturov AD, Golovko LF, Podchernyaeva IA (1986) Laser and electro-erosion hardening of the materials. Nauka, Moscow (in Russian)
10. Kozlenkov AI, Belov YI, Bogdanov VG, Shulgin AI (1981) Light element analysis and ultra soft X-ray spectroscopy with the use of electron microprobe. In: Proc 5th Microprobe Conf, Leipzig, pp 47–50
11. Lyakishev NP, Dyomina EV, Ivanov LI *et al.* (1996) Prospect of development and manufacturing of low activation metallic materials for fusion reactor. J Nucl Mater 233-237:1516–1522
12. Lyublinski IE, Dyomina EV, Evtichin VA *et al.* (1990) Effect of liquid Li on reduced-activation Cr-Mn steel. Fizika i Khimiya Obrabotki Materialov 3:131–137 (in Russian)
13. Maslyaev SA, Pimenov VN, Platov YM *et al.* (1998) Influence of deuterium plasma pulses generated in plasma focus device on the materials for thermonuclear fusion reactor. Perspektivnye Materialy 3:39–46 (in Russian)
14. Pleshivtsev NV, Bazhin AI (1998) Physics of interaction of ion beams with the materials. Vuzovskaya Kniga, Moscow (in Russian)
15. Sadowski M, Al-Mashhadani EM, Szydlowski A *et al.* (1994) Investigation on the response of CR-39 and PM-355 Track detectors to fast protons in the energy range 0.2–4.5 MeV. Nucl Instrum Meth Phys Res B 86:311–316
16. Scholz M, Miklaszewski R, Gribkov VA, Mezzetti F (2000) PF-1000 device. Nukleonika 45;3:155–158
17. Thomson M (1971) Defects and radiation damage in metals. Mir Publishers, Moscow (in Russian)
18. Umanskii YS, Skakov YA (1978) Physics of metals. Atomizdat, Moscow (in Russian)
19. Vertkov AV, Evtichin VA, Lyublinski IE *et al.* (1993) Mechanical properties of low activation Cr-Mn austenitic steel changes in liquid lithium. J Nucl Mat 203:158–163
20. Zabolotnyi VT, Lazorenko VM (1993) Cascades, sub-cascades and peaks of displacement in the tungsten after the irradiation by own ions. Fizika i Khimiya Obrabotki Materialov 3:17–22 (in Russian)
21. Zabolotnyi VT, Ivanov LI, Suvorov AL (1994) Field-ion microscopy and principal aspects of the radiation damage of the solid. Fizika i Khimiya Obrabotki Materialov 2:5–10